Karyometry of the Colonic Mucosa

David S. Alberts,[1] Janine G. Einspahr,[1] Robert S. Krouse,[1,2,7] Anil Prasad,[3] James Ranger-Moore,[1,5] Peter Hamilton,[8] Ayaaz Ismail,[4,7] Peter Lance,[1,4] Steven Goldschmid,[4] Lisa M. Hess,[1] Michael Yozwiak,[1] Hubert G. Bartels,[6] and Peter H. Bartels[1,6]

[1]Arizona Cancer Center and [2]Departments of Surgery, [3]Pathology, and [4]Medicine, College of Medicine; [5]College of Public Health; and [6]College of Optical Sciences, University of Arizona; [7]Southern Arizona Veterans Affairs Health Care System, Tucson, Arizona; and [8]Bioimaging and Informatics, Institute of Pathology, Queen's University, Belfast, United Kingdom

Abstract

Objective: **The study summarizes results of karyometric measurements in epithelial cells of the colorectal mucosa to document evidence of a field effect of preneoplastic development among patients with colorectal adenocarcinoma or adenoma.**

Methods: **Karyometric analyses were done on high-resolution images of histologic sections from 48 patients with colorectal adenocarcinomas and 44 patients with adenomas and on images from matching normal-appearing mucosa directly adjacent to such lesions, at a 1-cm and 10-cm distance from the lesions or from the rectal mucosa of adenoma patients, as well as from 24 healthy normal controls with no family history of colonic disease.**

Results: **The nuclei recorded in the histologically normal-appearing mucosa of patients with either colorectal adenoma or adenocarcinoma exhibited differences in karyometric features in comparison with nuclei recorded in rectal mucosa from patients who were free of a colonic lesion. These differences were expressed to the same extent in tissue adjacent to the lesions and in normal-appearing tissue as distant as the rectum.**

Conclusions: **The nuclear chromatin pattern may serve as an integrating biomarker for a preneoplastic development. The field effect might provide an end point in chemopreventive intervention trials.** (Cancer Epidemiol Biomarkers Prev 2007;16(12):2704–16)

Introduction

Colorectal cancer is the second most common cause of cancer death in United States (1). The concept that colorectal cancer develops through an adenoma-carcinoma sequence has long been held as the paradigm for colorectal cancer progression, although it is becoming increasingly clear that colorectal cancer is a more heterogeneous disease than had previously been recognized. Consequently, this paradigm must be expanded to include the recent knowledge gained from the enormous strides in the understanding of the colorectal cancer pathogenesis, especially in the area of molecular pathology (2). Colorectal cancer develops in a multistep manner over many years to decades with distinct benign and malignant stages of growth. Colorectal adenomas are routinely classified by size, histologic type, and degree of dysplasia, features that are associated with development of carcinoma within an adenoma. Additionally, adenoma size, multiplicity, and family history of colon cancer are associated with adenoma recurrence (3-5). Although removal of adenomas is associated with a lower risk of colorectal cancer, adenoma recurrence is a common event. Effective screening would likely prevent the majority of colorectal cancers through removal of the precursor lesion (6, 7). However, effective screening is limited by patient acceptance and adherence to recommended screening strategies. In 2000, it was estimated that <35% of the U.S. population adhered to colorectal screening recommendations (8).

Karyometry is a method of assessing nuclear chromatin pattern information that may be used to detect very early events in the carcinogenesis pathway (9). Therefore, karyometry offers a highly sensitive technique for the detection of changes concomitant with the progression of neoplastic disease. Nuclear chromatin patterns can be precisely measured by nuclear texture analysis—a computerized technique that measures the pixel gray values within a nucleus and computes the spatial and statistical relationships between these gray values. This can be achieved by high-resolution computerized image analysis. Previous studies have indicated that measures of nuclear chromatin organization by texture analysis provide a sensitive indicator of deviation from normality, which may precede changes in DNA content and is not apparent to the naked eye (10-13). The nuclear chromatin pattern has been shown to serve as an integrating biomarker (9) practically independent of specific pathways of progression. Changes in the nuclear chromatin pattern are reversible and they occur within a short time frame.

Furthermore, karyometry is capable of determining and statistically documenting changes in the chromatin pattern even if they occur in only a small proportion of nuclei (14). The ability to detect early cellular changes

Received 6/29/07; revised 9/4/07; accepted 10/4/07.

Grant support: NIH grants CA23074 and CA041108.

The costs of publication of this article were defrayed in part by the payment of page charges. This article must therefore be hereby marked *advertisement* in accordance with 18 U.S.C. Section 1734 solely to indicate this fact.

Requests for reprints: David S. Alberts, Arizona Cancer Center, College of Medicine, University of Arizona, 1515 North Campbell Avenue, Tucson, AZ 85724-5024. Phone: 520-626-7685; Fax: 520-626-2445. E-mail: dalberts@azcc.arizona.edu

doi:10.1158/1055-9965.EPI-07-0595

Table 1. Characteristics of nuclear chromatin from the rectal mucosa of individuals with colorectal adenomas, from colorectal adenomas, and from colorectal adenocarcinomas (Belfast series)

Chromatin feature	Rectal mucosa (SD)	Adenoma (SD)	Adenocarcinoma (SD)
Total absorbance	0.216 (0.110)	0.283 (0.131)	0.331 (0.222)
Nuclear area	14.1 (5.21)	25.1 (9.48)	29.2 (12.0)
Co-occurrence	0.212 (0.231)	0.478 (0.344)	0.543 (0.34)
Run length	5.162 (9.09)	25.7 (24.8)	31.81 (25.44)
Nonuniform absorbance	17.6 (7.22)	30.8 (14.3)	31.07 (12.3)
Relative no. runs	169.7 (71.4)	279.6 (164.4)	311 (155.4)
No. median absorbance pixels	508.2 (253.6)	911.8 (432.5)	939.3 (545.8)

may enable clinicians to detect precancerous changes before they are visible by histopathologic evaluation, which makes karyometry a potential method of assessing the effectiveness of chemopreventive agents to prevent progression to cancer.

A recent karyometric study of normal-appearing rectal mucosa from 129 patients with a history of adenoma showed that the nuclear chromatin pattern offers clues to the risk of recurrence of a colonic lesion and suggests that observed changes in the nuclear chromatin pattern represent a preneoplastic development (15). The observation of preneoplastic changes in the rectal or colonic mucosa was not unexpected. In 1990, Bibbo and colleagues at the University of Chicago (11, 16) had reported measurable changes in the chromatin pattern of nuclei immediately adjacent to and at 5, 10, 20, and 50 mm from colonic adenocarcinoma in histologically normal-appearing mucosa. Earlier studies, such as those by Filipe and Branfoot (17) and Dawson and Filipe (18), had reported histochemical changes in the mucosa adjacent to and remote from colonic carcinoma. Riddell and Levin (19) found ultrastructural changes in the mucosa adjacent to carcinoma of the colon. Saffos and Rhatigan (20) described light microscopic changes in mucosa adjacent to colonic cancer and Shamsuddin et al. (21) described changes in the colonic mucosa adjacent to and remote from cancer of the colon.

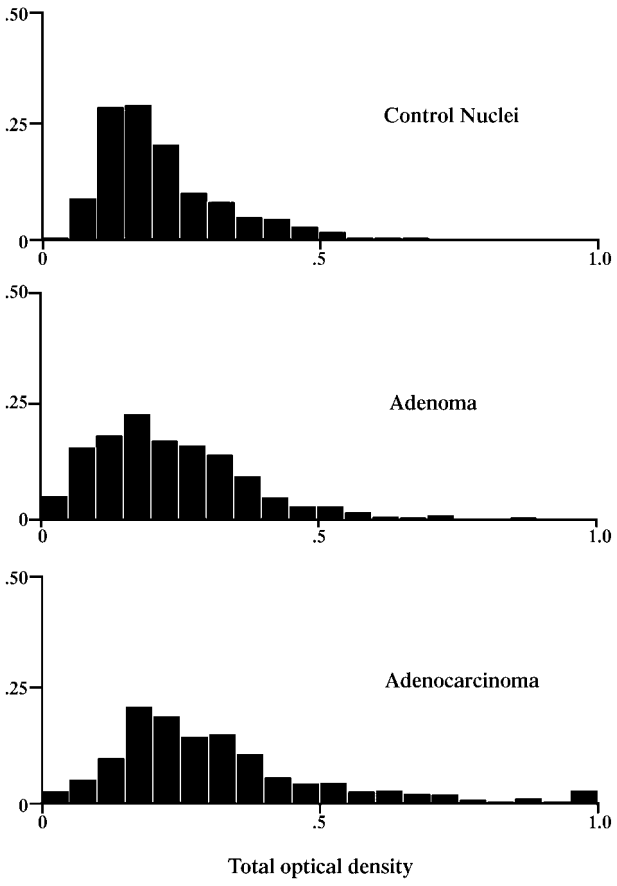

Figure 1. Distribution of total absorbance (*optical density*) values in rectal mucosa from individuals with colorectal adenomas, colorectal adenoma, and colorectal adenocarcinoma (Belfast series).

Terpstra et al. (22) reported increases in the uptake of thymidine and increased cell proliferation along the entire colon in patients with neoplastic colonic disease. They referred to this effect as ''a proliferative lesion'' and proposed using thymidine uptake as a screening method for people at risk for the development of colon neoplasia or ''for the evaluation of measures aimed at reducing that risk'' (i.e., chemopreventive intervention).

Ngoi et al. (23), by the use of flow cytometry, reported aneuploidy in normal-appearing colonic mucosa up to 10 cm distant from colorectal cancers. These authors considered their findings of aneuploidy and a high S-phase fraction in uninvolved superficial colonic mucosa as evidence for a field effect in mucosa adjacent to colorectal cancer.

The current study was designed to document the expression of preneoplastic changes in patients with colorectal lesions (i.e., adenoma or adenocarcinoma) and individuals with no evidence of colorectal polyps using standardized karyometric methods in laboratories at the University of Arizona Cancer Center (Tucson, Arizona) and Queen's University (Belfast, United Kingdom).

Materials and Methods

Belfast Data Set. The first data set (recorded in Belfast) included a subset of 20 participants enrolled to the Arizona Cancer Center's Wheat Bran Fiber Study (24). Eligible Wheat Bran Fiber Study participants included individuals between the ages of 40 and 80 years, who had had one or more histologically confirmed colorectal adenomas removed within 6 months of study enrollment (designated as the qualifying adenoma), which were used in this analysis. Samples were obtained from the adenoma lesion, from histologically normal-appearing tissue adjacent (1 cm) from the lesion, and, subsequently,

Table 2. Discriminant function (DF I,1) values for selected features from rectal mucosa of individuals with colorectal adenomas and from colorectal adenocarcinomas (Belfast series)

Chromatin feature	Rectal mucosa	Adenocarcinoma	Standardized coefficient
Nuclear area	14.1	29.2	0.666
Average staining density	38.3	27.7	−0.647
Run length	169.7	311.0	0.262
No. lightly stained pixels	162.6	459.7	−0.143

rectal mucosal biopsies were obtained 8 to 12 cm above the anal verge before the start of the study intervention. In addition, the data recorded in Belfast included samples collected from 19 colorectal cancer patients. Biopsy samples were taken at the time of surgery from the lesion, within 1 cm adjacent to the lesion, and at a distance of ~10 cm or at the distant edge of the resection.

Tucson Data Set. A second data set was recorded in Tucson and included 24 individuals who underwent colonoscopy with at least one adenoma ≥8 mm. Biopsies were obtained from the largest adenoma, mucosa within 1 cm of the adenoma, and rectal mucosa 8 to 12 cm from the anal verge. The Tucson data set also included 29 patients with adenocarcinoma. Biopsies were obtained during surgery from the carcinoma, from normal-appearing mucosa within 1 cm of the carcinoma, and from distant, normal-appearing mucosa at ~10 cm or at the distant edge of the resection. Twenty-four healthy patients undergoing a screening colonoscopy with no personal or family history of colorectal disease and with no evidence of colorectal polyps provided rectal mucosal biopsy samples that served as normal controls.

All biopsies were collected during colonoscopy or surgery for colorectal cancer at the Arizona Health Sciences Center and the Southern Arizona Veterans Affairs Health Care System, Tucson, Arizona. Each study was approved by the Institutional Review Board of the University of Arizona and/or Southern Arizona Veterans Affairs Health Care System and all subjects provided written informed consent.

All biopsy materials were fixed in 10% neutral buffered formaldehyde. Tissue sections were cut to 5 μm and stained with H&E. Data were recorded in Tucson on a videophotometer equipped with a 100:1, 1.40-numerical aperture plan apochromatic oil immersion objective from Nikon. Data in Belfast were recorded with a 100:1 oil immersion objective. The sampling density was adjusted by relay optics to 6 pixels per linear micron at both locations.

Each image was segmented and 100 nuclear profiles stored digitally for texture computation. A total of 95 texture features are computed on each nucleus relating to the spatial and statistical distribution of gray values within the nucleus. This was carried out using the TICAS software (Optical Sciences Center, University of Arizona, Tucson, AZ). The computation of chromatin texture features was furthermore used to define a nuclear signature, which reflects the unique chromatin characteristics of a given nucleus.

Karyometric Analysis

The use of 95 karyometric features captures chromatin information at varying levels of complexity. Most of the features fall into one of three broad categories, each of which summarizes information at increasingly higher order. Features of zero-order statistics are based on the values of all pixels in the nucleus, such as the total absorbance, the mean absorbance, absorbance variance, and relative nuclear area (total number of pixels). Features based on first-order statistics are derived from individual pixels, such as the relative frequency of occurrence of pixel absorbance values. Features descriptive of second-order statistics are based on the relationship of a pixel and its immediately adjacent neighbor, such as the similarity or difference of absorbance value. These features are known as co-occurrence values. Features descriptive of higher-order statistics include run lengths. A run is a sequence of pixels along the scan line in the digitized image, all falling within a certain absorbance range. The number of runs of different lengths and in different absorbance ranges provides a set of features. Finally, there are features descriptive of the local arrangement of multiple pixels of given gray values: chromatin condensation (referred to as pixel absorbance condensation); chromatin or pixel absorbance clumpness; and pixel absorbance heterogeneity and homogeneity (25). The full set of features captures a broad range of information that maximizes the opportunity to detect nuclear changes of significance in cancer

Table 3. Classification matrices

	Rectal mucosa* vs adenocarcinoma		Rectal mucosa* vs adenoma		Normal control rectal mucosa vs adenocarcinoma		Normal control rectal mucosa vs adenoma	
	DF (I,1)		DF (I,2)		DF (I,3)		DF (I,4)	
	Wilks' Λ = 0.496		Wilks' Λ = 0.61		Wilks' Λ = 0.641		Wilks' Λ = 0.784	
	Rectal mucosa	Adenocarcinoma	Rectal mucosa	Adenoma	Rectal mucosa	Adenocarcinoma	Rectal mucosa	Adenoma
Rectal mucosa	85.5%	14.5%	84.8%	15.2%	92.7%	7.3%*	75.6%	24.4%
Adenocarcinoma	10.5%	89.5%	21.5%	78.5%	33.9%	66.1%	32.7%	67.3%

*Rectal mucosal samples were obtained from participants with adenoma.

Table 4. Training set and test set

	Normal control rectal mucosa vs adenocarcinoma			
	DF I,3 (Wilks' Λ = 0.701)			
	Training set		Test set	
	Rectal mucosa	Adenocarcinoma	Rectal mucosa	Adenocarcinoma
Rectal mucosa	90.9%	9.1%	92.3%	7.7%
Adenocarcinoma	35.4%	64.6%	33.7%	66.3%
Accuracy	76.9%		79.3%	

progression. Typically indicative of such progression is an increase in total absorbance, an increase in the relative nuclear area, an increases in run lengths, or denser staining pixels.

Nuclear Signature. The nuclear signature was obtained by first calculating the mean and SD of each karyometric feature in nuclei from a normal reference tissue (e.g., rectal mucosa from healthy individuals). For the nuclear signature, the value of each feature in the tissue under study was standardized relative to the normal reference tissue. This was done by computing the absolute difference in value for each feature between the reference and the study nuclei, and standardizing this difference by dividing it by the SD of each feature as found for the reference nuclei. This indicates, for each feature, how many normal-tissue SDs away from the normal-tissue value each nucleus lies. The numerical value for each feature is a z value. For the 95 features, the result is a nuclear signature, graphed as a bar chart. The features are arranged in an arbitrary but consistent fashion, with the vertical height of each bar depicting the deviation from normal. A nuclear signature may be computed for an individual nucleus or it can be averaged across all nuclei in a sample. In normal tissue, the height of each bar is $\sim$0.65, which is the typical mean absolute deviation in a Gaussian distribution. Tissues experiencing progression to cancer show marked increases in z value for numerous karyometric features (26).

The Lesion Signature. Averaging the z values across all 95 standardized features in each nucleus results in a measure of nuclear abnormality. Plotting the relative frequency histogram of nuclear abnormality for all nuclei recorded for a lesion produces the lesion signature. Progression to cancer is revealed as a positive skew in the lesion signature because progression is accompanied by increasing numbers of nuclei deviating notably from normal. The average nuclear abnormality, computed as the mean over the abnormality values of all nuclei in a sample from a given lesion, is a useful measure of lesion progression (16, 26).

The Discriminant Function. Development of a discriminant function (DF) is based typically on a small number (e.g., four to eight) of those karyometric features that are best able to distinguish between normal and abnormal tissues. It provides a method even more sensitive than the lesion signature for detecting treatment effects in cancer chemoprevention studies. The development of a DF is a form of supervised learning, in which the diagnostic category of each nucleus is used in DF generation. To choose the appropriate karyometric features without imposing distributional assumptions, a nonparametric Kruskal-Wallis test was used. In addition, a low significance level of $p < 0.005$ was used in light of the multiple comparisons being conducted. Four to eight of the karyometric features showing strong differences between the two tissue types were then submitted to a discriminant algorithm and the resulting discriminant function was applied to samples from the study.

Results

Biopsy samples were provided from 116 study participants. These samples were measured in two series, one in Belfast, United Kingdom, at Queens University, and the second in Tucson, Arizona, at the University of Arizona Cancer Center.

Belfast Data Set. The Belfast data included 19 patients with colorectal adenocarcinoma and 20 patients with colorectal adenoma. In the adenocarcinoma lesions, 595 nuclei were recorded. In the histologically normal-appearing mucosa, 923 nuclei were recorded adjacent to the adenocarcinoma lesion (1 cm from the lesion) and 956 nuclei were recorded at a location 10 cm distant from the adenocarcinoma lesion. In the adenoma lesion, 558 nuclei were recorded. In addition, 845 nuclei were

Table 5. Discriminant function mean values

Sample	Mean (DF I,1)	Mean (DF I,2)	Mean (DF I,3)	Mean (DF I,4)
Rectal mucosa	−0.917*	−0.839*	−0.493†	−0.4709,† −0.442*
Normal appearing, distant from lesion	−0.697	−0.578	−0.127	
Normal appearing, adjacent to lesion	−0.643	−0.518	−0.136	−0.3085
Adenoma	+0.249	+0.440		+0.4577
Adenocarcinoma	+0.517	+0.772	+0.728	

*Rectal mucosal samples were obtained from participants with adenoma.
†Rectal mucosal samples from normal healthy controls (norm/norm).

Table 6. Proportion of nuclei deviant from normal

Sample	DF I,1 (%)	DF I,2 (%)	DF I,3 (%)
Rectal mucosa	14.2	12	7.3
Normal appearing, distant from lesion	28.3	31	28.5
Normal appearing, adjacent to lesion	32.1	34	35.8
Adenoma	70.9	89	N/A
Adenocarcinoma	85.5	100	66.1

Abbreviation: N/A, not available.

recorded in the histologically normal-appearing rectal mucosa of the patients with adenoma. There were no controls from healthy individuals in this study. The counts reflect all nuclei pooled across cases.

Tucson Data Set. The Tucson data included 29 patients with colorectal adenocarcinoma, 24 patients with colorectal adenoma, and 24 patients with no evidence or history of disease (healthy controls). For the carcinoma cases, there were 2,748 nuclei recorded in the carcinoma region, 3,016 nuclei in the adjacent locations, and 3,012 nuclei at distant locations. For the adenoma cases, there were 6,965 nuclei recorded, 2,403 of which were from the adenoma, 2,301 adjacent to the lesions, and 2,261 at a distant location in the histologically normal-appearing rectal mucosa. In addition, biopsies from the healthy controls contributed a total of 2,336 control nuclei.

Nuclear Chromatin Patterns

Belfast. A number of characteristics of the nuclear chromatin undergo a monotonic change in value from normal to colorectal carcinoma, as seen in Table 1 for some selected variables, from the material processed in Belfast. All feature values are given in relative arbitrary units. The total absorbance distribution underwent a shift from normal mucosa to adenoma and onto adenocarcinoma, toward higher values, as seen in Fig. 1.

A discriminant analysis (DF I,1) for the rectal mucosal nuclei from adenoma patients versus adenocarcinoma was carried out. The nuclear area, average staining density, run length, and number of densely stained pixels in the nucleus were selected as features. Nuclear area and average staining density carried the greatest weights. Table 2 shows the values for these features.

Wilks' Λ, as the test statistic for the group separation in the discriminant analysis, was reduced to 0.496. The four features listed in Table 2 were included in the function. The average correct classification rate was 86.9%. The classification matrices for the subsequent discriminant analyses DF I,2, DF I,3, and DF I,4 are given in Tables 3 and 4. When applied to nuclei recorded distant from and adjacent to the carcinoma lesions, the mean discriminant function values given in Table 5 were obtained.

The nuclei recorded in the histologically normal-appearing tissue, both at the distant and at the adjacent locations, were distinctly different from those recorded in the rectal mucosa. The changes, as expressed by the mean discriminant function scores, suggest a progression toward abnormality. If one considers the discriminant function score as an indicator of deviation from normal, the proportion of nuclei not assigned to the normal diagnostic category also expresses the preneoplastic development. Table 6 lists these proportions.

To see whether a discriminant function anchored at the rectal mucosa versus the adenoma samples, which have a slightly different feature set, might provide a better separation of the nuclei recorded in the distant biopsies among carcinoma patients, a second discriminant function DF I,2 was derived. This function used only three features: relative nuclear area, pixel absorbance variance, and the number of dark stained pixels in the nucleus. Wilks' Λ was reduced to 0.61. The classification matrix shown in Table 3 was obtained, with an average correct classification rate of 80.6%. The mean discriminant function DF I,2 scores for all sampling locations, including the carcinoma region, are presented in Table 5. The gain was modest.

The classification rates reported in Table 3 reflect differences in the chromatin pattern for the nuclei in different diagnostic categories. For the data recorded in Belfast, the percentages of nuclei classified as showing a deviation from normal for the different sampling locations are listed in Table 6. The adjacent and distant location data suggest a definitive change or preneoplastic development.

Tucson. To separate nuclei from normal control rectal mucosa from nuclei from colorectal cancer, a discriminant function DF I,3 was derived in the following manner. The cases of normal controls, from patients free of any colorectal disease and referred to as norm/norm, were randomly divided into two data sets. One of these sets was to serve as training set and the other as validation or test set for the classification. The same was done to the cases from colorectal cancer. Feature selection for the training sets identified seven chromatin texture features as having high discrimination potential. The discrimination run for the training set resulted in the classification matrix shown in Table 4 and had an average accuracy of 76.9%. The classification rule was then applied to the test set and the classification results are presented in Table 4. The average accuracy was

Table 7. Discriminant function (DF I,3) values for selected features from normal and adenocarcinoma biopsies

Chromatin feature	Rectal mucosa, healthy controls	Adenocarcinoma	Standardized coefficient
Total absorbance	0.475	0.854	0.603
Pixel absorbance inhomogeneity	17.61	31.45	−0.435
No. median absorbance pixels	518	1,018	0.431
Nuclear area	14.8	26.99	−0.324
Run percentage	332	582	−0.194
Run length feature	11.7	18.3	0.190
Pixel absorbance ranging from 1.3 to 1.4	14.8	19.6	−0.156

79.3%. Given the excellent agreement, the same set of features was next applied to a discriminant function for the combined set, resulting in an average correct classification rate of 79.4%, and reported as the results for DF I,3.

The seven chromatin features are listed in Table 7, together with their values for both the norm/norm and the adenocarcinoma data sets. Also given are the standardized coefficients for the discriminant function DF I,3. Wilks' Λ was reduced to 0.641.

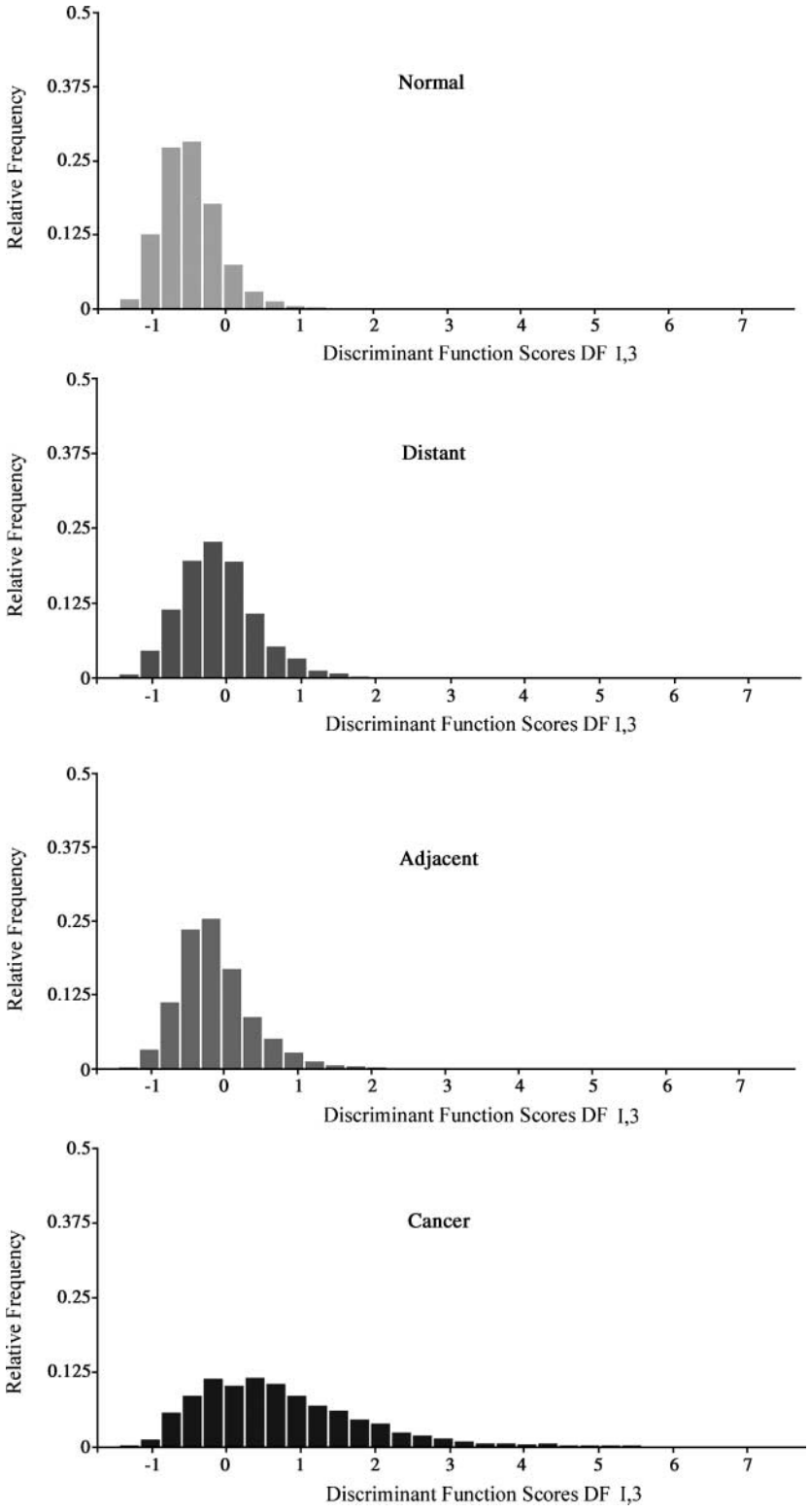

Figure 2. Distributions of discriminant function DF I,3 scores for rectal mucosa from individuals with no evidence of colorectal polyps at colonoscopy, mucosa distant from and adjacent to adenocarcinoma, and in the carcinoma lesion (Tucson series).

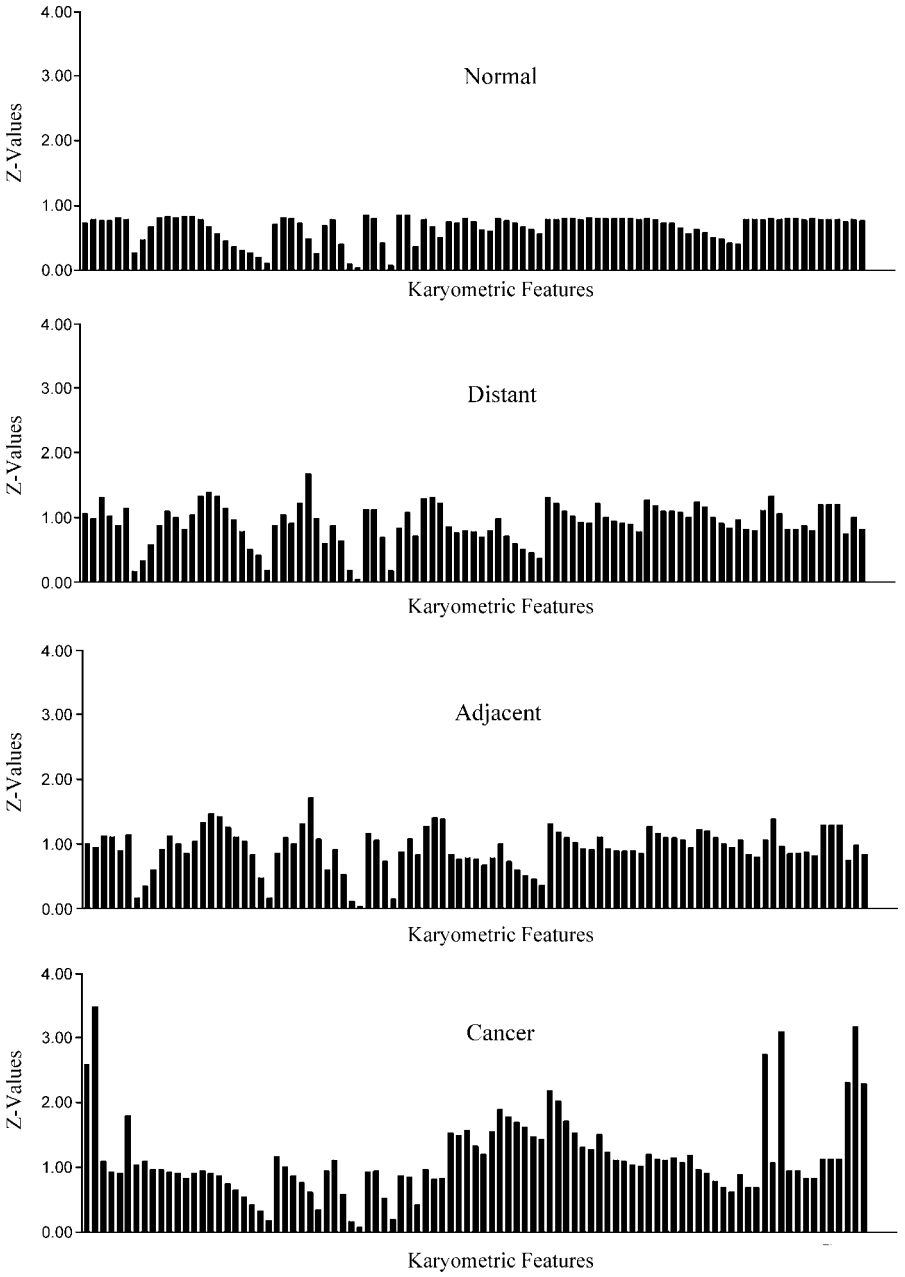

Figure 3. Nuclear signatures for nuclei sampled in rectal mucosa from individuals with no evidence of colorectal polyps at colonoscopy, mucosa distant from and adjacent to adenocarcinoma, and in the carcinoma lesion (Tucson series).

A number of nuclei in the region of the lesion were classified as near normal. Our protocol for measurement specifies that nuclei, within the region outlined as ''lesion,'' be selected at random.

Applied to the samples at locations distant to and adjacent to the carcinoma lesions, the discriminant function distributions DF I,3 seen in Fig. 2 were obtained. For both the distant and the adjacent sampling locations, a small shift in score values toward abnormality is observed. The shift is similar for both of these sampling locations.

The discriminant function DF I,3 mean values for all sampling sites are listed in Table 5. For the Tucson adenoma data, a corresponding discriminant function (DF I,4) was developed. It used seven features: the number of medium absorbance stained pixels, nuclear roundness, relative nuclear area, pixel absorbance heterogeneity, pixel absorbance condensation, total absorbance, and long run emphasis. Wilks' Λ was reduced to 0.784. The overall correct classification rate was 71.4%. The discriminant function mean score values are given in Table 5 for the sampling locations in the norm/norm rectal mucosa, in the normal-appearing rectal mucosa of patients with adenoma as a distant sample, in the normal-appearing mucosa 1 cm adjacent to an adenoma lesion, and in the adenoma lesion. The progression curve is seen in Fig. 9.

The nuclei sampled in the histologically normal-appearing mucosa in both the Tucson and Belfast data show evidence of a preneoplastic development. Evidence

for such a development was also observed in the nuclear signatures, as seen in Fig. 3. Figure 4 shows the lesion signatures for the data recorded in Tucson. These signatures represent the distributions of nuclear abnormality for all nuclei sampled at a sampling location. Table 8 shows the monotonic increase in average nuclear abnormality. The lesion signatures for the nuclei recorded in the histologically normal-appearing mucosa extend to higher deviations than seen in the rectal control (norm/norm) sample.

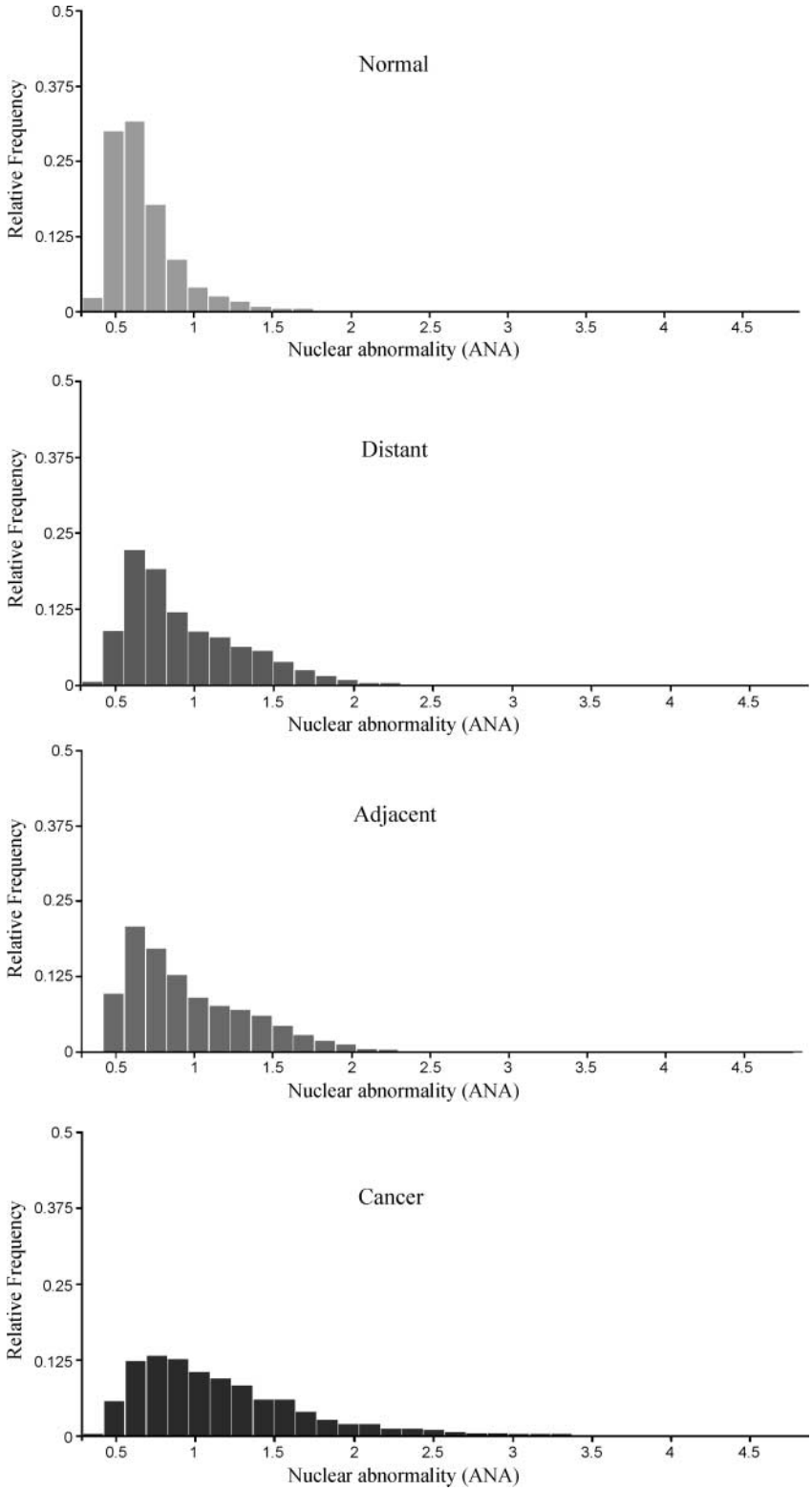

Figure 4. Distribution of averaged nuclear abnormality values average nuclear abnormality (lesion signatures) for rectal mucosa from individuals with no evidence of colorectal polyps at colonoscopy, mucosa distant from and adjacent to an adenocarcinoma, and the carcinoma lesion (Tucson series).

Table 8. Average nuclear abnormality

Sample	Average nuclear abnormality
Rectal mucosa, healthy controls	0.67
Normal appearing, distant from carcinoma	0.92
Normal appearing, adjacent to carcinoma	0.94
Adenoma	1.08
Adenocarcinoma	1.16

Returning to the discriminant function score distributions for the different diagnostic categories, the values recorded in Belfast are shown in Fig. 5. In this figure, the absolute number of nuclei recorded is plotted on the ordinate. The proportion of nuclei with a discriminant function score >0 is shown in Table 9.

The distributions of nuclear abnormality values (i.e., the lesion signatures) show an almost identical trend. Here, a direct comparison of values from the Belfast and the Tucson series of measurements was possible because nuclear signatures and lesion signatures are tied to internal references and thus insensitive to differences in staining protocol. For a population of normal nuclei, the expected nuclear abnormality is 0.65. Figure 4 shows that a threshold set at the average nuclear abnormality of 0.70 would set aside any nuclei with even a slight deviation from normal. Such a threshold separates out a fair number of almost normal nuclei and is therefore very conservative. Figure 4 also shows that the great majority of nuclei exceeding this threshold deviate from normal by <1 SD (averaged over all 95 features).

If one tabulates the proportion of cases from both the Tucson and Belfast data with a certain percentage of nuclei in the average nuclear abnormality range >0.70 as a function of diagnostic category, the plot in Fig. 6 is obtained. The ordinate in Fig. 6 is formed by the proportion of cases. The abscissa was formed by the proportion of nuclei falling into the average nuclear abnormality range >0.70 (i.e., all nuclei with feature values ranging from just slightly above normal to nuclei deviating by several SDs). Figure 6 shows that in adenoma, 20% of the cases have from 20% to 30% of their nuclei in the range >0.70 average nuclear abnormality. Only 4.8% of normal cases have more than 50% of their nuclei in the average nuclear abnormality range >0.70, as compared with 90.7% of cases with adenocarcinoma.

In both Tucson and Belfast data, the progression from rectal mucosa to colorectal adenocarcinoma consistently followed a similar trend. Figure 7 shows the progression curve obtained from the DF I,1 scores of the Belfast series plotted against total absorbance. Shown are the mean values for each diagnostic group and the 95% confidence ellipses for the nuclear data. The measurements taken in normal-appearing colon tissue adjacent to (norm/Ca adj.) and distant from (norm/Ca dist.) a carcinoma lesion show a preneoplastic development and are found between rectal mucosa and adenoma at ~10% of the distance from normal to carcinoma. As a reminder, the rectal mucosa controls in this plot stemmed from patients with adenoma (norm/adenoma, rectal).

In the adenocarcinoma nuclei recorded in Tucson, the measurements taken in the normal-appearing colonic tissue adjacent to and distant from the carcinoma lesion fall into a near linear line of progression from normal to

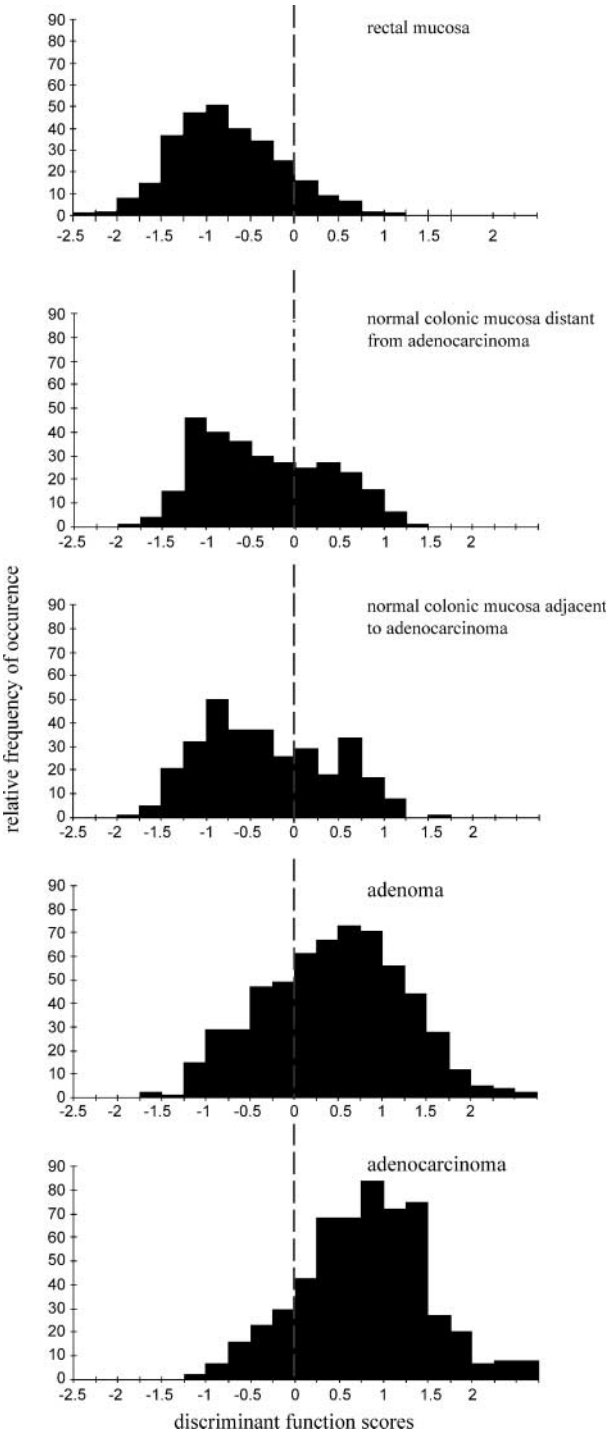

Figure 5. Absolute frequency distributions for discriminant function scores recorded in rectal mucosa from individuals with colorectal adenomas, mucosa distant from and adjacent to colorectal adenocarcinoma, colorectal adenoma, and colorectal adenocarcinoma (Belfast series).

Table 9. Proportion of nuclei with discriminant function score >0

Sample	Proportion with DF score >0 (%)
Rectal mucosa, healthy controls	8
Normal appearing, distant from carcinoma	26
Normal appearing, adjacent to carcinoma	27
Adenoma	69
Adenocarcinoma	82

adenocarcinoma, as seen in Fig. 8. Here, the 95% confidence ellipses for the mean values are much smaller due to the larger sample sizes.

In the adenoma samples, the displacement due to preneoplastic change was notably smaller but still statistically significant. This is seen in Fig. 9, where the discriminant function DF I,4 score was plotted against total absorbance.

The differences in staining protocol made it inadvisable to compare feature values directly between Tucson and Belfast. However, it was possible to plot data from different data sets on a relative scale (e.g., based on the difference in mean value for the norm/norm data and the carcinoma data, as a scale from 0 to 100).

Such a plot shows the progression of nuclear change in colorectal lesions, as shown in Fig. 10, with the relative scale as ordinate and total absorbance as abscissa. Here, the 95% confidence ellipses for the case mean values are shown. One may describe the progression not only as a curve but as a 95% confidence envelope, as shown in Fig. 10. Preneoplastic development involves small but notable changes in feature values. In H&E-stained material from Belfast and Tucson series, the changes range from 15% to 20% (Fig. 10).

Discussion

There are two aspects to the interpretation of the statistical results. First, there is the test of the hypothesis that measurements taken in histologically normal-appearing colonic mucosa of patients with neoplastic lesions yield results that are statistically significantly different from measurements taken in normal control colonic tissue. As seen in Fig. 7, the 95% confidence

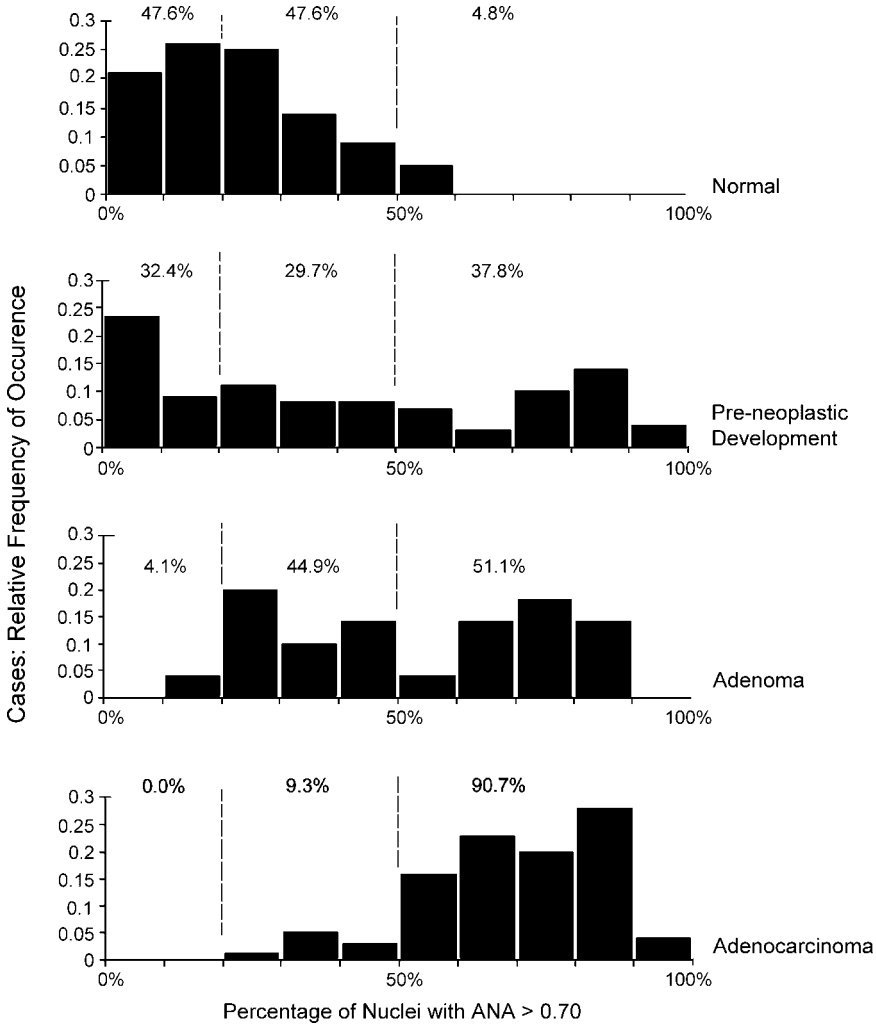

Figure 6. Relative frequency distributions of cases with a certain percentage of nuclei in the average nuclear abnormality range >0.70 (Tucson and Belfast series).

ellipses for measurements taken in the normal-appearing colonic mucosa of patients with adenocarcinoma do not overlap with that of the rectal mucosa measurements taken as a reference in the Belfast data set.

The same is true for the measurements of the Tucson data set taken from patients with adenocarcinoma. Here, the confidence ellipses do not overlap with those for the normal control measurement series. There was no difference between measurements taken adjacent to and at a distance from the adenocarcinoma lesion. For the measurements taken in the Tucson data set from patients with adenoma, the reference data were taken from the rectal mucosa of healthy normal cases, but the distant sampling site was in the histologically normal-appearing rectal mucosa 10 cm from the anal verge. Again, the 95% confidence ellipses for the off-lesion sampling sites are very close, but they do not overlap and the difference is thus significant at $p < 0.05$.

All of the above results are based on mean and confidence limits computed across all nuclei at each sampling site. The large sample sizes allow the detection of very small differences as statistically significant. Although one always ought to weigh the sensitivity of detection against what one might consider as biologically significant, the observed differences hold up for the 95% confidence ellipses computed for the distributions of case means as seen in Fig. 10. Thus, the hypothesis that a preneoplastic development occurs in the colonic mucosa of patients with neoplastic lesions can be accepted.

However, for a clinical application, these statistics are of little use. Here, not the confidence ellipse for a mean computed across a number of cases is relevant but the value observed in an individual case and a statistic such as the tolerance ellipse for the case mean distribution. The tolerance ellipse defines the region into which a certain percentage of case means are expected to decrease, for instance, 90% of cases.

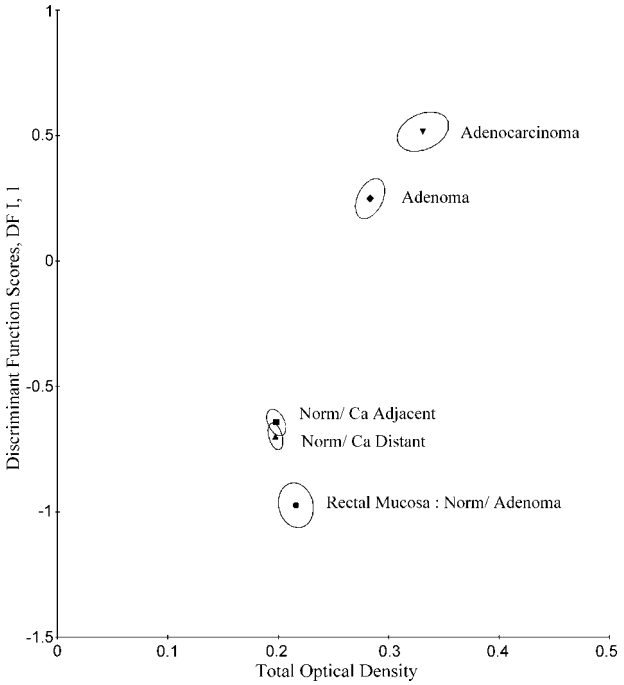

Figure 7. Progression curve for colonic lesions based on discriminant function DF I,1 and total absorbance (Belfast series).

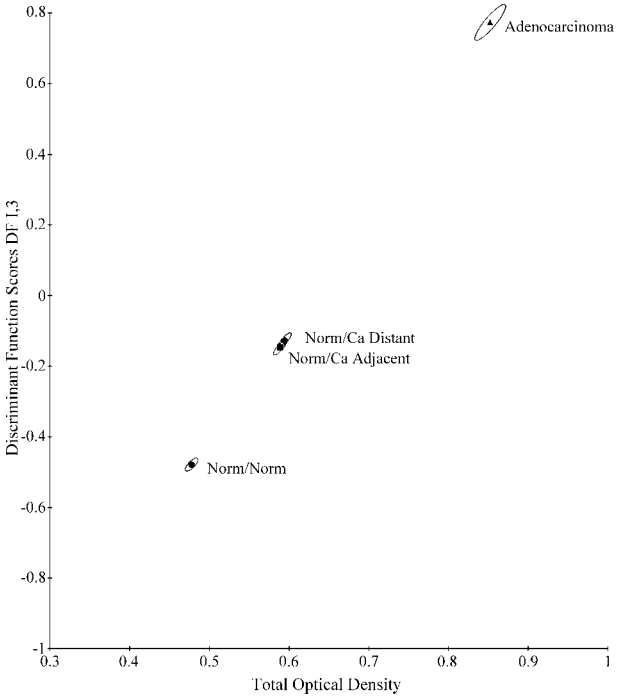

Figure 8. Progression curve for colonic lesions based on discriminant function DF I,3 and total absorbance (Tucson series).

Two sources of variation affect such a region. One is the case-to-case variation. It is of the same magnitude as the differences due to preneoplastic development. For the features used in the DF I,3 function, the case-to-case coefficient of variation for the norm/norm cases ranged from 11.5% to 18.4%. For the data sets taken from the sampling sites off-lesion, the coefficients of variation ranged from 17.0% to 20.5%. For karyometric measurements, these coefficients of variation are not substantial. However, whereas the data sets in this study were too small to allow a definitive conclusion, they may rule out the use of case mean discriminant function scores in a screening application due to lack of specificity. The percentage of nuclei with high nuclear abnormality may provide a better criterion.

The second source of variation is differences between different biopsies taken from the same patient. A brief study was carried out involving 25 individuals, with triplicate, randomly placed biopsies taken from each in the rectal mucosa. For the karyometric features used (e.g., in the DF I,3 function), the difference in value from the mean across the triplicate biopsies ranged from 5% to 11%.[9]

In the application of karyometry to a chemoprevention clinical trial, the latter source of variation sets the critical

[9] H. Bartels, personal communication 2007.

limit for the detection of efficacy. The case-to-case variation here is not entered due to the baseline and end-of-study biopsies collected from each individual in such a study.

In this study, there was a reassuring consistency in the data recorded in different institutions and with different staining protocols. This holds true as compared with historical data collected in the 1990s. The total absorbance increase for nuclei from normal mucosa and from adenocarcinoma was measured in 1990 in Chicago at 85% (11, 16), and in this study it was 80%. This consistency remains despite the fact that materials were processed in different laboratories following different staining protocols and different video microphotometers were used. The earlier measurements carried out in Chicago had shown changes in the histologically normal-appearing colorectal mucosa in cases with adenocarcinoma. The analysis of these data had concentrated on the immediate vicinity of the margin of the lesion, from <1 mm to 1 cm, and then been extended to 50 mm. It had been found that the proportion of nuclei deviating substantially from normal gradually declined over that distance, but that even at the 50-mm distant location, several percent of the sampled nuclei showed clear signs of progression. At that time, no effort had been made to document the subtle chromatin changes characteristic for preneoplastic development.

The cause and exact nature of the preneoplastic changes in the nuclear chromatin are still unknown. In 1965, when Nieburgs et al. (27) described visually apparent changes in nuclei adjacent to and distant from malignant tumors—the so-called malignancy associated changes—they speculated that these might be a manifestation of an abnormal premitotic stage. The changes

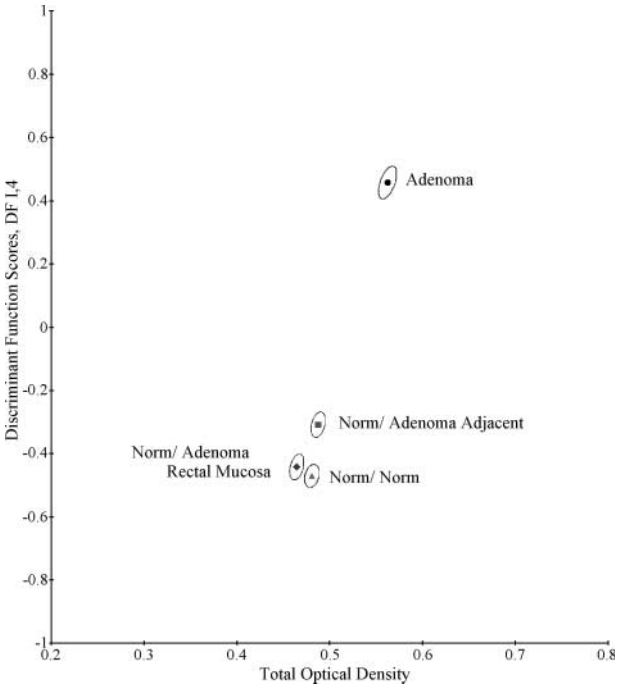

Figure 9. Progression curve for colonic lesions based on discriminant function DF I,4, and total absorbance (Tucson series).

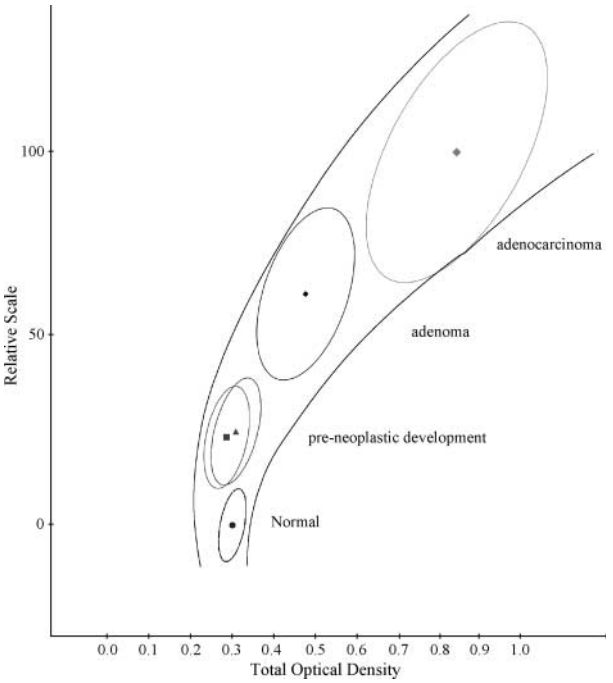

Figure 10. Progression of colonic lesions based on a relative scale derived from different discriminant functions and total absorbance. Shown are the bivariate means, the 95% confidence ellipses for the case means, and a 95% confidence envelope for case means.

observed in the rectal mucosa described here are not visually apparent. It is possible that they reflect an early stage in redifferentiation that eventually may lead to neoplasia and malignant transformation, indicated by the concomitant heterochromatinization (28). Heterochromatin formation is the result of abundant aberrant hypermethylation in certain CpG islands (29). It leads to epigenetic silencing by sequestration of genes into transcriptionally repressed nuclear neighborhoods (30). An association between karyometric measures of chromatin organization and methylation/histone acetylation has recently been shown for prostatic intraepithelial neoplasia and adenocarcinoma (31) and for the colon.[10]

Efforts to develop agents effective in the chemoprevention of neoplastic lesions of the colorectal mucosa would be greatly aided by methods allowing a quantitative numerical determination of their effects. Karyometry can detect and statistically secure changes too subtle to be detected by visual inspection in histologically normal-appearing colonic mucosa and in normal-appearing rectal mucosa far distant from a lesion.

Thus, procedures to document efficacy of a chemopreventive agent based on karyometric measurement of a reversal of progressive change lend themselves ideally to the purpose. To establish suitable procedures for the colonic mucosa, it is necessary to define a ''progression curve.'' This will allow a numerical assessment of the

[10] P.W. Hamilton, personal communication 2007.

state of progression of colonic tissue at any point between normal and adenocarcinoma. In a chemoprevention clinical trial, one has the advantage of observing the difference between within-case baseline biopsies and end-of-study biopsies. A limitation of the use of karyometric methods to detect chemopreventive efficacy in individual cases is sampling variability. A study for estimates of sampling variability is under way.

Despite these limitations, this study shows that normal-appearing rectal mucosa from participants with adenoma or adenocarcinoma is not ''normal'' as measured by karyometry. This study shows that in the colon, there is a clear field defect that extends to adjacent, distant, and rectal mucosa among participants with an adenoma or adenocarcinoma lesion present. Thus, in chemoprevention trials, changes in chromatin patterns as far as the rectum may serve as a biomarker of response throughout the colon.

References

1. Jemal A, Siegel R, Ward E, Murray T, Xu J, Thun, MJ. Cancer statistics, 2007. CA Cancer J Clin 2007;57:43–66.
2. Day DW, Morson BC. The adenoma-carcinoma sequence. Major Probl Pathol 1978;10:58–71.
3. Morson B. President's address. The polyp-cancer sequence in the large bowel. Proc R Soc Med 1974;67:451–7.
4. Muto T, Bussey HJ, Morson BC. The evolution of cancer of the colon and rectum. Cancer 1975;36:2251–70.
5. Winawer SJ, Zauber AG, Gerdes H, et al. National Polyp Study Workgroup. Risk of colorectal cancer in the families of patients with adenomatous polyps. N Engl J Med 1996;334:82–7.
6. Winawer SJ, Zauber AG, Ho MN, et al. Prevention of colorectal cancer by colonoscopic polypectomy. The National Polyp Study Workgroup. N Engl J Med 1993;329:1977–81.
7. Muller AD, Sonnenberg A. Prevention of colorectal cancer by flexible endoscopy and polypectomy. A case-control study of 32,702 veterans. Ann Intern Med 1995;123:904–10.
8. Subramanian S, Klosterman M, Amonkar MM, Hunt TL. Adherence with colorectal cancer screening guidelines: a review. Prev Med 2004; 38:536–50.
9. Bartels PH, Ranger-Moore J, Alberts D, Hess L, Scarpelli M, Montironi R. Carcinogenesis and the hypothesis of phylogenetic reversion. Anal Quant Cytol Histol 2006;28:243–52.
10. Bartels PH, daSilva VD, Montironi R, et al. Chromatin texture signatures in nuclei from prostate lesions. Anal Quant Cytol Histol 1998;20:407–16.
11. Bibbo M, Michelassi F, Bartels PH, Dytch H, Bania C, Lerma E, Montag AG. Karyometric marker features in normal-appearing glands adjacent to human colonic adenocarcinoma. Cancer Res 1990;50:147–51.
12. Bartels PH, Montironi R, Hamilton PW, Thompson D, Vaught L, Bartels HG. Nuclear chromatin texture in prostatic lesions. I. PIN and adenocarcinoma. Anal Quant Cytol Histol 1998;20:389–96.
13. Bartels PH, Montironi R, Thompson D, Vaught L, Hamilton PW. Statistical histometry of the basal cell/secretory cell bilayer in prostatic intraepithelial neoplasia. Anal Quant Cytol Histol 1998;20: 381–8.
14. Bartels PH, Ranger-Moore J, Stratton MS, et al. Statistical Analysis of chemopreventive efficacy of Vitamin A in sun-exposed, normal skin. Anal Quant Cytol Histol 2002;24:185–97.
15. Ranger-Moore J, Frank D, Lance P, et al. Karyometry in rectal mucosa of patients with previous colorectal adenomas. Anal Quant Cytol Histol 2005;27:134–42.
16. Montag AG, Bartels PH, Dytch HE, Lerma-Puertas E, Michelassi F, Bibbo M. Karyometric features in nuclei near colonic adenocarcinoma. Statistical analysis. Anal Quant Cytol Histol 1991;13: 159–67.
17. Filipe ML, Branfoot AC. Abnormal patterns of mucus secretion in apparently normal mucosa of large intestine with carcinoma. Cancer 1974;34:282–90.
18. Dawson PA, Filipe ML. An ultrastructural and histochemical study of the mucous membrane adjacent to and remote from carcinoma of the colon. Cancer 1976;37:2388–98.
19. Riddell RH, Levin B. Ultrastructure of the ''transitional'' mucosa adjacent to large bowel carcinoma. Cancer 1977;40:2509–22.
20. Saffos RO, Rhatigan RM. Benign (nonpolypoid) mucosal changes adjacent to carcinomas of the colon. A light microscopic study of 20 cases. Hum Pathol 1977;8:441–9.
21. Shamsuddin AK, Weiss L, Phelps PC, Trump BF. Colon epithelium. IV. Human colon carcinogenesis. Changes in human colon mucosa adjacent to and remote from carcinomas of the colon. J Natl Cancer Inst 1981;66:413–9.
22. Terpstra OT, van Blankenstein M, Dees J, Eilers GA. Abnormal pattern of cell proliferation in the entire colonic mucosa of patients with colon adenoma or cancer. Gastroenterology 1987;92: 704–8.
23. Ngoi SS, Staiano-Coico L, Godwin TA, Wong RJ, DeCosse JJ. Abnormal DNA ploidy and proliferative patterns in superficial colonic epithelium adjacent to colorectal cancer. Cancer 1990;66: 953–9.
24. Alberts DS, Martinez ME, Roe DJ, et al. Lack of effect of a high-fiber cereal supplement on the recurrence of colorectal adenomas. Phoenix Colon Cancer Prevention Physicians' Network. N Engl J Med 2000; 342:1156–62.
25. Young T, Verbeek PW, Mayall B. Characterization of chromatin distributions in cell nuclei. Cytometry 1986;7:467–74.
26. Ranger-Moore J, Alberts DS, Montironi R, et al. Karyometry in the early detection and chemoprevention of intraepithelial lesions. Eur J Cancer 2005;41:1875–88.
27. Nieburgs HE, Parets AD, Perez V, Boudreau C. Cellular changes in liver tissue adjacent and distant to malignant tumors. Arch Pathol 1965;80:262–72.
28. Harbers E, Sandritter W. [Increased heterochromatization as a pathogenetic principle]. Dtsch Med Wochenschr 1968;93:269–71.
29. Egger G, Liang G, Aparicio A, Jones P. Epigenetics in human disease and prospects for epigenetic therapy. Nature 2004;429:457–63.
30. Cheutin T, McNairn A, Jenuwein T, Gilbert D, Singh P, Misteli T. Maintenance of stable heterochromatin domains by dynamic HP1 binding. Science 2003;299:721–5.
31. Mohamed MA, Greif PA, Diamond J, et al. Epigenetic events, remodelling enzymes and their relationship to chromatin organization in prostatic intraepithelial neoplasia and prostatic adenocarcinoma. BJU Int 2007;99:908–15.

Karyometry of the Colonic Mucosa

David S. Alberts, Janine G. Einspahr, Robert S. Krouse, et al.

Cancer Epidemiol Biomarkers Prev 2007;16:2704-2716.